Carbohydrate Polymers 261 (2021) 117879

Contents lists available at ScienceDirect

Carbohydrate Polymers

journal homepage: www.elsevier.com/locate/carbpol

Structural characterization and antioxidant activities of one neutral polysaccharide and three acid polysaccharides from *Ziziphus jujuba* cv. *Hamidazao*: A comparison

Yanmin Yang [a,1], Zhichang Qiu [a,1], Lingyu Li [a], Sriram K. Vidyarthi [b,c], Zhenjia Zheng [a], Rentang Zhang [a,*]

[a] College of Food Science and Engineering, Shandong Agricultural University, 61 Daizong Street, Tai'an, 271018, Shandong, PR China
[b] Department of Biological and Agricultural Engineering, University of California, Davis, 95616, CA, USA
[c] Research and Development, The Morning Star Company, Woodland, 95695, CA, USA

ARTICLE INFO

Keywords:
Ziziphus jujuba cv. *Hamidazao*
Polysaccharide
Structural characterization
Antioxidant
Comparison

ABSTRACT

A neutral polysaccharide (HJP-1a) and three acid polysaccharides (HJP-2, HJP-3 and HJP-4) were obtained from *Z. jujuba* cv. *Hamidazao*. HJP-1a was mainly composed of arabinose and galactose in a ratio of 56.9:20.0, with an average molecular weight of 3.115×10^4 g/mol. HJP-2, HJP-3 and HJP-4 were homogeneous heteropolysaccharides mainly containing galacturonic acid, arabinose and galactose, with average molecular weights of 4.590×10^4, 6.986×10^4 and 1.951×10^5 g/mol, respectively. Structural characterization indicated that the backbone of HJP-3 appeared to be mainly composed of →4)-*α*-D-Gal*p*A (1→ and →2,4)-*α*-L-Rha*p* (1→ residues with some branches consisting of →5)-*α*-L-Ara*f* (1→ residues and terminals of T-*α*-L-Ara*f* (1→ and T-*β*-D-Gal*p* residues. The four purified fractions displayed dose-dependent radical scavenging activity on $ABTS^+$ radicals and reducing capacity, as well as excellent protective effect on H_2O_2-induced HepG2 cells and metronidazole-damaged zebrafish embryos, especially HJP-2 *in vitro* and HJP-1a *in vivo*. Therefore, the polysaccharides from *Z. jujuba* cv. *Hamidazao* could be used as a potential antioxidant in functional foods.

1. Introduction

Jujube (*Ziziphus jujuba* Mill.), belonging to the genus *Ziziphus* and the family *Rhamnaceae*, has been extensively used as a health food and medicinal herb (Ji et al., 2017). As one of the most valuable fruits, jujube contains abundant nutrients: polysaccharides, proteins, fatty acids, polyphenols, vitamins, minerals, organic acids and other active ingredients (such as saponins) (Wang et al., 2018; Wojdylo, Carbonell-Barrachina, Legua, & Hernandez, 2016). According to ancient Chinese books of herbal medicine, jujube is considered sweet and warm, and contributes to nourishing the body, improving sleep quality, regulating the human digestive system and extending the life-span (Chen et al., 2013). Modern pharmacological studies have confirmed that jujube is beneficial to multiple disorders and diseases, such as fatigue, anemia, inflammation, diabetes, cancer and cardiovascular diseases (Gao, Wu, & Wang, 2013; Ji et al., 2017).

Polysaccharides are natural high-molecular polymers formed by diverse monosaccharides and their derivatives linked with different glycosidic bonds. They dominate the bioactive components of jujube fruits and are responsible for multiple health benefits (Chang, Hsu, & Chen, 2010; Ji, Liu, Peng, & Wang, 2018; Lin et al., 2018). Therefore, increasing attention has been paid to the polysaccharides from jujube fruits due to their higher bioactivity and relatively lower toxicity. Nowadays, jujube polysaccharides with various physiochemical and structural features have been extracted, purified and characterized from multiple *Ziziphus jujuba* Mill. (*Z. jujuba*) varieties. Based on multiple spectroscopic and chromatographic techniques, a neutral polysaccharide (the main backbone composed of Ara*f* and Glc*p* with branches at O-3 and O-5) and three acidic polysaccharides: PZMP3-2 (the main backbone composed of 1,4-Gal*p*A residues with branches at O-2), PZMP2-2 (the main backbone composed of (1→4)-linked Gal*p*A and (1→2,4)-linked Rha*p* residues, with branches at O-4) and SAZMP3 (the main backbone composed of 1,4-*α*-Gal*p*A with side chains of 1, 3-*β*-D-Gal*p*, 1,3,5-linked Ara*f* and 1,2,4-*α*-L-Rha*p*) have been obtained

* Corresponding author.
E-mail address: rentangzhang@163.com (R. Zhang).
[1] These authors contributed equally to this work.

https://doi.org/10.1016/j.carbpol.2021.117879
Received 1 October 2020; Received in revised form 6 February 2021; Accepted 25 February 2021
Available online 1 March 2021

and characterized from *Z. Jujuba* cv. *Muzao* (Ji et al., 2018; Ji et al., 2019; Ji, Yan, Hou, Shi, & Liu, 2020; Lin, Ji, Wang, Yin, & Peng, 2019). Furthermore, Li, Fan, and Ding (2011) and Li, Ai, Yang, Liu, and Shan (2013) respectively reported a water-soluble polysaccharide: ZSP3c from *Z. jujuba* cv. *Jinsixiaozao* (the backbone consisting mainly of (1→4)-*α*-D-Gal*p*A and (1→2)-*α*-L-Rha*p* with branches attached at O-4 of the rhamnosyl residues) and ZP2a from *Z. jujuba* cv. *Junzao* (the backbone consisting mainly of 1,4-D-Gal*p*A, 1,2-L-Rha*p* and 1,2,4-L-Rha*p* residues with branches at O-4 position of Rha*p* residues). Therefore, the structural and physicochemical properties of polysaccharides vary greatly among different *Z. jujuba* varieties. The nutritional and health value of *Z. jujuba* cv. *Hamidazao* ranks among the top jujubes in the word due to special climatic conditions. However, there is no report on the extraction, purification and structural characterization of the polysaccharides from *Z. jujuba* cv. *Hamidazao*. We conjectured that the polysaccharides from *Z. jujuba* cv. *Hamidazao* differed from those from other jujube varieties and they were bio-macromolecules composed of multiple fractions with different structures and health benefits. Therefore, it is quite necessary to comparatively analyze the profile, structure and biological activity of different polysaccharides from *Z. jujuba* cv. *Hamidazao*.

The aim of this study was to comparatively investigate the structural characteristics of different polysaccharide fractions from *Z. jujuba* cv. *Hamidazao* based on ultraviolet-visible (UV–vis) spectroscopy, high-performance gel permeation chromatography coupled with multi-angle laser light scattering and refractive index detector (HPGPC-MALLS/RID), Fourier transform infrared-attenuated total reflection (FTIR-ATR) spectrometry, high-performance anion-exchange chromatography coupled with pulsed amperometric detector (HPAEC-PAD), methylation analysis and nuclear magnetic resonance (NMR) spectroscopy. Furthermore, the antioxidant activity of different purified polysaccharides was analyzed by experiments *in vitro* and *in vivo*. The results would provide comparative information on the structure and biological activity of different polysaccharide fractions from *Z. jujuba* cv. *Hamidazao* and demonstrated their potential as novel antioxidants in the functional food and pharmaceutical industries.

2. Materials and methods

2.1. Materials

Z. jujuba cv. *Hamidazao* fruits were purchased from Tai'an wholesale Market (Shandong, China). Monosaccharide standards (mannose, ribose, rhamnose, glucose, galactose, xylose, arabinose, fucose, fructose, glucuronic acid and galacturonic acid), DEAE-cellulose 52, and Sephadex G-100 were obtained from Shanghai Yuanye Bio-Technology Co. Ltd (Shanghai, China). Acetonitrile, trifluoroacetic acid (TFA) and trypsin were purchased from Sigma-Aldrich (St. Louis, MO, USA). Cell Counting Kit-8 (CCT-8) and DMEM/HIGH Glucose medium were provided by Shanghai Biyuntian Bio-Technology Co., Ltd (Shanghai, China) and Gibco Life Technologies (Waltham, MA, USA), respectively. Dimethyl sulfoxide (DMSO), metronidazole (MET), hydrogen peroxide (H_2O_2) and Vitamin C (Vc) were purchased from Beijing Solarbio Technology Co., Ltd. (Beijing, China). All other reagents were of analytical grade.

2.2. Extraction, purification and fractionation of polysaccharides

The jujube fruits were pitted and sliced, followed by drying at 60 ℃ and crushing with a high-speed disintegrator. The sieved powder (425 μm) of jujube fruits was subjected to polysaccharide extraction with distilled water at a ratio of 1:10 (*w/v*) for 45 min twice. After the supernatant was filtered and concentrated by a rotary evaporator at 60 °C, the crude polysaccharides were obtained by precipitation with the 4-fold volume of absolute ethanol and centrifugation at 1790 *g* for 10 min. Then, the obtained polysaccharide solutions (50 mg/mL) were defatted with petroleum ether and deproteinized with Sevag reagent (chloroform: butyl alcohol = 4:1, *v/v*). After precipitation again with ethanol, the purified crude polysaccharides were freeze-dried for fractionation.

3 g of crude polysaccharides of *Z. jujuba* (HJP) were dispersed in 100 mL of distilled water and filtered through a 0.45 μm membrane, and then applied to a DEAE-cellulose 52 anion-exchange column (5.0 × 100.0 cm). The distilled water and a stepwise gradient NaCl aqueous solution (0.1, 0.2 and 0.3 mol/L) were used for elution at a flow rate of 5.0 mL/min. The polysaccharide fractions were collected and monitored by the phenol-sulfuric acid method at 490 nm (Nielsen, 2010). Four fractions (named as HJP-1, HJP-2, HJP-3 and HJP-4) were obtained, concentrated and lyophilized for further purification. 50 mg of lyophilized polysaccharide powder was dissolved in 10 mL of distilled water and then loaded onto a Sephadex G-100 gel column (2.6 × 60.0 cm), which was eluted with distilled water at a flow rate of 0.6 mL/min and monitored by the phenol-sulfuric acid method. The main polysaccharide fractions were collected, concentrated, dialyzed with dialysis tubes (500–1000 Da) against distilled water for 48–72 h, and lyophilized for structural and biological analysis.

2.3. Physicochemical property of polysaccharides

The protein content was determined using the Bradford method with bovine serum albumin as the reference (Bradford, 1976). The phenolic compound content was analyzed according to the method of Vázquez et al. (2015).

2.4. Structural characterization of polysaccharides

2.4.1. UV–vis spectroscopy

The UV–vis spectra of four polysaccharide solutions at 1 mg/mL were recorded in the range of 200–400 nm using a UV-2450 spectrophotometer (Shimadzu, Japan). Each sample was scanned three times.

2.4.2. Molecular weight determination

The weight-average molecular weight (Mw) distribution and polydispersity (Mw/Mn) of the four polysaccharide fractions were determined by HPGPC-MALLS/RID (Wyatt-DAWN HELEOS-II, USA) according to the method proposed by Wu et al. (2019a). The polysaccharide powder was prepared as the 2 mg/mL aqueous solution and then filtered through a 0.22 μm millipore filter. An aliquot of 20 μL sample solution was injected and analyzed using Shodex SB-806 HQ gel column (300.0 × 7.8 mm) at a flow rate of 0.5 mL/min and a column temperature of 40 °C, with 0.1 mol/L $NaNO_3$ as mobile phase. During the measurement, the value of dn/dc (specific refractive index increment) was set at 0.145 mL/g. The Astra 5.3 software (Wyatt Technology Corp., USA) was used to calculate the molecular weight distribution.

2.4.3. Monosaccharide composition analysis

The monosaccharide composition of jujube polysaccharides was determined by HPAEC-PAD (Thermo Fisher ICS-5000$^+$, USA). Briefly, the hydrolysis of polysaccharide powder (10 mg) was conducted in a test tube containing 2 mL of TFA at 100 °C for 6 h, followed by rotary evaporation for the removal of the residual TFA. After the sample volume was adjusted to 10 mL with ultra-pure water, the purification was performed on the Supelclean™ ENVI-18 SPE tube (500 mg/6 mL) (Supelco, USA) and a 0.22 μm millipore filter. The analysis was performed using Dionex™ AminoPac™ PA10 IC column (Dionex, 3 × 250 mm) as follows: 0.20 mol/L NaOH solution and 1.00 mol/L NaAc solution as mobile phase, 30 °C of column temperature, 0.25 mL/min of flow rate. The identification and quantification of different sugars were achieved respectively by comparing the retention time and peak area with those of monosaccharide standards (rhamnose, arabinose, galactose, glucose, mannose, xylose, fructose, galacturonic acid and glucuronic acid).

2.4.4. FTIR spectroscopy analysis

3 mg of dried polysaccharide powder was placed in the sample stage. The FTIR-ATR spectra were produced by a Thermo Nicolet IS10 FTIR spectrophotometer equipped with a universal ATR (Thermo Fisher Scientific Inc., USA). After the background spectrum of air was deducted, the scanning was performed from the mid-IR mode in the range of 4000 to 400 cm^{-1} at a resolution of 4 cm^{-1}, in triplicate. The comparison and annotation of absorption peaks were performed using OMNIC 8.2 software.

2.4.5. Methylation analysis of HJP-3

As described by Yuan et al. (2015), HJP-3 was subjected to methylation analysis because it was the most abundant component in HJP. Briefly, 10 mg of HJP-3 was dissolved in 1 mL of ultrapure water and reacted with 1 mL of 100 mg/mL carbodiimide for 2 h. After the mixture reacted with 1 mL of 2 mol/L imidazole and 1 mL of 30 mg/mL of $NaBD_4$ for 3 h, 100 μL of glacial acetic acid was added to terminate the reaction. The obtained sample was dialyzed for 48 h and lyophilized for methylation. The reduced polysaccharide sample was dissolved in DMSO, and reacted with NaOH for 30 min. Then, the methylation was conducted using methyl iodide for 1 h, followed by extraction with dichloromethane and drying by a stream of nitrogen. After the obtained methylated product was hydrolyzed with 2 M TFA at 121 °C for 90 min, reduced by 1 mol/L $NaBD_4$ and acetylated with acetic anhydride at 100 °C, the analysis of acetylated derivatives was performed on gas chromatograph-mass spectrometer (Agilent 7820 A-5977, Agilent, Santa Clara, CA, USA). The detailed procedures were shown in the supplementary data.

2.4.6. NMR analysis

20 mg of polysaccharide sample was repeatedly dissolved in 0.5 mL D_2O three times and then transferred to a NMR tube. The NMR spectra were recorded on a high-resolution AVANCE III 400 NMR spectrometer (Bruker, Germany) at 25 °C. One-dimensional NMR spectra (^1H and ^{13}C) and two-dimensional NMR spectra (correlation spectroscopy [COSY], heteronuclear single quantum coherence [HSQC] and heteronuclear multiple bond coherence [HMBC]) were adopted to analyze the structural features of polysaccharides (Wu et al., 2019b).

2.5. Antioxidant activity in vitro

The four polysaccharide fractions were prepared as aqueous solutions at the concentrations of 0, 0.2, 0.4, 0.6, 0.8 and 1.0 mg/mL. $ABTS^+$ radical scavenging activity was analyzed as described by Raguraman et al. (2019) and Zhang et al. (2017), and the total reducing power was evaluated according to the method of Gao, Wang, Wang, and Wang (2013).

The antioxidant activity of polysaccharides was further evaluated by H_2O_2-induced HepG2 cell viability using CCK-8 kit (Xu, Qiao, Guo, Ma, & Cheng, 2018). The HepG2 cells frozen in liquid nitrogen were first activated three times, followed by adjustment to 50,000 cells/mL with complete medium. After treatment with 0.25 % trypsin, an aliquot of 100 μL HepG2 cells was transferred in a 96-well culture plate (Corning, NY, USA) at 37 °C for 12 h in a humidified atmosphere containing 5 % CO_2. Subsequently, the medium solution in each well was replaced with 100 μL of polysaccharide solutions at the concentrations of 25, 50 and 100 μg/mL (dissolved in DMEM high-glucose medium containing 0.5 % DMSO) for experimental group. Vc (100 μg/mL) was analyzed as positive control, and DMEM high-glucose medium was used for negative control. After incubation at 37 °C for 12 h, the H_2O_2 solution was added to each well (except the blank group) at a final concentration of 12 mmol/L for 12 h. Finally, an aliquot of 10 μL reagents from CCK-8 kit was added and incubated for 2 h, and the optical density at 450 nm ($OD_{450\ nm}$) was measured using a Cytation™5 cell imaging and microplate reader (Bio-Tek, USA).

2.6. Antioxidant activity in vivo

Ten adult zebrafish provided by the Biology Institute of Shandong Academy of Sciences were kept in a 3-L acrylic tank at 28 °C and provided with *Artemia salina* as feed three times per day, with a 14 h of light in the room. After the zebrafish were placed at a female to male ratio of 1:2 for 1 d, the embryos were naturally collected within 30 min, which was induced by lighting in the morning. The obtained healthy embryos at about 24 h post-fertilization (hpf) were divided into 18 groups (6–8 embryos in each group) and transferred into individual well of a 24-well plate containing embryo medium (with 1 mL of 0.1 % DMSO). Different concentrations of polysaccharide solutions (5, 25 and 50 μg/mL) and 5 mmol/L MET were added into the plate of the experimental groups, and only 5 mmol/L MET was applied to the negative control group, with Vc used as the positive control. After incubated at 28.5 °C for 24 h, the embryos were imaged by a fluorescence microscopy (Olympus IX51, Japan). The number of fluorescence points was quantified by spectrofluorimetry using Image pro-plus.

2.7. Statistical analysis

All experiments were repeated three times except for the determination of molecular weight, expressed as the mean ± standard deviation. The significance of differences was assessed using one-way analysis of variance (ANOVA) combined with the Turkey' test by SPSS software at $P < 0.001$, $P < 0.01$ and $P < 0.05$.

3. Results and discussion

3.1. Extraction, purification and fractionation of polysaccharides

The *Z. jujuba* cv. *Hamidazao* polysaccharides were obtained *via* hot-water extraction and preliminary purification, with a yield of 2.3 ± 0.5 % on the basis of dry matter. After the fractionation by the DEAE-cellulose 52 column, one neutral polysaccharide (HJP-1) and three acid polysaccharides (HJP-2, HJP-3 and HJP-4) were produced, with the recovery rates of 30.0 %, 3.8 %, 18.7 % and 5.2 %, respectively (Fig. 1A). The elution profile was similar to that of crude polysaccharides from *Z. jujuba* cv. *Jinsixiaozao* and *Z. jujuba* cv. *Muzao* (Ji et al., 2018; Li et al., 2011), and the number of obtained fractions was more than that of crude polysaccharides from *Z. jujuba* cv. *Huizao* (Zou, Chen, Sun-Waterhouse, Zhang, & Li, 2018). Further purification using Sephadex G-100 column indicated that HJP-2, HJP-3 and HJP-4 displayed a single and symmetrical peak, respectively. Although two components appeared in the elution profile of HJP-1, the second fraction (HJP-1b) disappeared during dialysis (Fig. 1B). Therefore, a total of four fractions, HJP-1a (with a yield of 16.8 %), HJP-2, HJP-3 and HJP-4, were used for structural characterization and bioactivity analysis. UV–vis spectrum (Fig. S1) and Bradford method (with 0.24 %, 0.35 %, 0.11 % and 0.26 % proteins, respectively) showed that these four polysaccharide fractions contained very little proteins. The total phenol content was significantly reduced from 1.5 % in HJP to 0.12 %, 0.14 %, 0.01 % and 0.08 % in HJP-1, HJP-2, HJP-3 and HJP-4, respectively. Furthermore, the neutral polysaccharide (HJP-1a) had the smallest Mw (3.115×10^4 Da), while the values of the three acid polysaccharides (HJP-2, HJP-3 and HJP-4) were 4.590×10^4 Da, 6.986×10^4 Da and 1.951×10^5 Da, respectively, based on HPGPC-MALLS/RID chromatogram. The different Mws in the range of 10^4–10^6 Da were observed for various *Z. jujuba* fruits, which was related to the variety, extraction, separation and purification procedures (Ji et al., 2017; Li et al., 2011; Li et al., 2013; Wu et al., 2019b).

3.2. Monosaccharide composition

As shown in Table 1, HJP-1a was mainly composed of arabinose, galactose, xylose and glucose in a ratio of 56.9:20.0:8.7:8.5, indicating

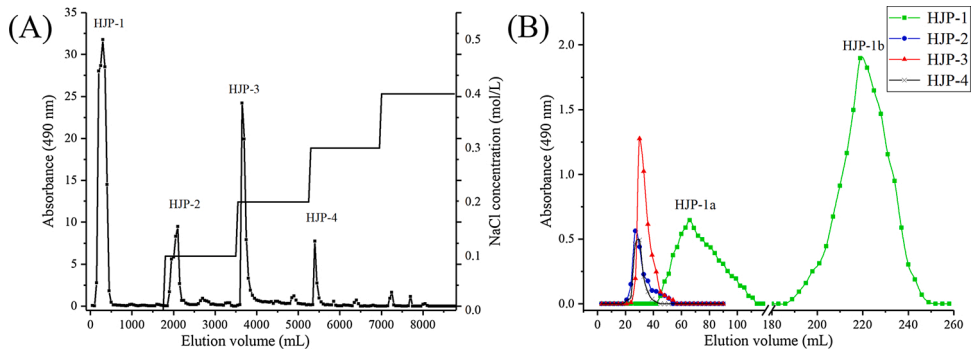

Fig. 1. Isolation and purification of crude polysaccharides and four fractions from *Z. jujuba* cv. *Hamidazao* fruits. (A) The elution profile of crude *Z. jujuba* cv. *Hamidazao* polysaccharides on the DEAE-52 cellulose column. (B) The elution curve of four components (HJP-1a, HJP-2, HJP-3 and HJP-4) on the Sephadex G-100 column (2.6 × 60.0 cm, total volume of 391.9 cm^3 and void volume of 106.1 cm^3).

Table 1
Physicochemical property, molecular weight and monosaccharide composition of four purified polysaccharide fractions from *Z. jujuba* cv. *Hamidazao* fruits.

	HJP-1a	HJP-2	HJP-3	HJP-4
Physicochemical property				
Protein content (%)	0.24 ± 0.02	0.35 ± 0.07	0.11 ± 0.01	0.26 ± 0.02
Total phenol content (%)	0.12 ± 0.01	0.14 ± 0.00	0.01 ± 0.00	0.08 ± 0.01
Molecular weight				
Mw (g/mol)	3.115 × 10^4	4.590 × 10^4	6.986 × 10^4	1.951 × 10^5
Mw/Mn	1.442	3.582	1.491	3.542
Monosaccharide composition				
Rhamnose (%)	–	0.56 ± 0.04	9.81 ± 0.12	2.24 ± 0.01
Arabinose (%)	56.93 ± 0.31	16.52 ± 0.13	24.15 ± 0.17	30.91 ± 0.12
Galactose (%)	19.99 ± 0.11	10.74 ± 0.05	10.97 ± 0.04	7.60 ± 0.09
Glucose (%)	8.45 ± 0.12	0.49 ± 0.02	0.20 ± 0.01	0.29 ± 0.04
Mannose (%)	3.76 ± 0.02	0.26 ± 0.01	0.24 ± 0.00	–
Xylose (%)	8.67 ± 0.08	0.25 ± 0.01	0.83 ± 0.02	0.19 ± 0.00
Fructose (%)	1.84 ± 0.02	0.82 ± 0.01	–	1.78 ± 0.00
Galacturonic acid (%)	0.37 ± 0.00	70.36 ± 0.32	53.80 ± 0.21	56.98 ± 0.23

The data were expressed as mean ± standard deviation. The percentage of monosaccharides was based on all detected monosaccharides.

that arabinose was the dominant monosaccharide in neutral polysaccharides of *Z. jujuba* cv. *Hamidazao* fruits. All three acid polysaccharides were proved to be heteropolysaccharides, which contained almost the same kind of neutral monosaccharides (rhamnose, arabinose, galactose, glucose, mannose, xylose and fructose) and acid monosaccharide (galacturonic acid) but in different mass ratios. Galacturonic acid was an abundant monosaccharide in HJP-2, accounting for a total of 70.4 % of all monosaccharides. There was also some arabinose and galactose, with a percentage of 27.3 %. The level of galacturonic acid ranked first in HJP-3 with an average of 53.8 %, followed by arabinose (24.2 %), galactose (11.0 %) and rhamnose (9.8 %). Although other monosaccharides were also detected but with low abundance (less than 1.0 %). Similar to HJP-3, HJP-4 had a higher proportion of galacturonic acid (57.0 %) and arabinose (30.9 %), and the lower proportion of galactose (7.6 %), rhamnose (2.2 %) and fructose (1.8 %), as well as trace amounts of glucose (0.29 %) and xylose (0.19 %). Therefore, the monosaccharide profiles of the four polysaccharides had significant differences. Ji et al. (2018) and Ji et al. (2020) reported that a neutral polysaccharide from *Z. jujuba* cv. *Muzao* consisted of arabinose, galactose, glucose, mannose and xylose in the molar ratio of 17.4:3.3:2.7:1.1:1.0 (mass ratio of 17.4:4.0:3.2:1.3:1.0), while a galacturonic acid-rich polysaccharide was composed of rhamnose, arabinose, galactose and galacturonic acid in a molar ratio of 1.7:2.0:1.0:18.7 (mass ratio of 1.6:1.7:1.0:20.1). The differences in jujube varieties, production conditions and determination methods could partially explain these discrepancies (Li et al., 2013; Lin et al., 2018; Lin et al., 2019).

3.3. FTIR-ATR spectral analysis

FTIR spectra revealed the main functional groups of polysaccharides. As presented in Fig. 2, a strong absorption peak at 3200.0–3400.0 cm^{-1} was ascribed to the O—H stretching vibration of intramolecular or intermolecular hydrogen bonds, while the weak absorption band at around 2940.0 cm^{-1} was attributed to the asymmetric stretching vibration of C—H, including the CH, CH_2, and CH_3 groups (Tian, Zhao, Zeng, Zhang, & Zheng, 2016). Some differences were observed in the absorption intensities of the four polysaccharides at these two characteristic wavelengths (Liu et al., 2020). The strong absorbance peaks at around 1738.0 cm^{-1} for HJP-3 and HJP-4, along with the weak bands in the range of 1235.0–1258.0 cm^{-1} for HJP-2, HJP-3 and HJP-4, were due to the stretching vibration of C═O in the ester or carboxyl groups, indicating the presence of uronic acids (Tian et al., 2016; Vasilieva et al., 2017). The result was consistent with the monosaccharides composition. There were significant peaks at 1600.0–1650.0 cm^{-1} and 1400.0–1420.0 cm^{-1} in four polysaccharides, which were derived from symmetrical C═O stretching vibrations and asymmetrical C═O stretching vibrations coupled C—H bending vibrations, respectively (Vasilieva et al., 2017). Furthermore, the C—O—H and C—O—C structural arrangements produced the vibration absorption in the range of 1000.0–1200.0 cm^{-1}, where three/four absorption bands appeared in HJP-3 and HJP-4 but only one existed in HJP-1a and HJP-2. The absorption peaks at 896.6 cm^{-1} and 833.9/833.1 cm^{-1} confirmed the presence of β-glycosidic bonds in HJP-1a and α-type glycosidic linkages in HJP-3 and HJP-4, respectively (Ren, Xu, Lu, & Yin, 2018; Zhang et al., 2016; Zou et al., 2018). Furthermore, there was a weak absorption peak at around 770.0 cm^{-1} for four polysaccharides. The FTIR spectra of these four jujube polysaccharide fractions were similar to those of the corresponding polysaccharides reported by Chang et al. (2010), indicating that they had similar structures.

3.4. Methylation analysis of HJP-3

The methylation analysis provides information on the structure of polysaccharides, such as the type and ratio of glycosidic bonds. Table 2

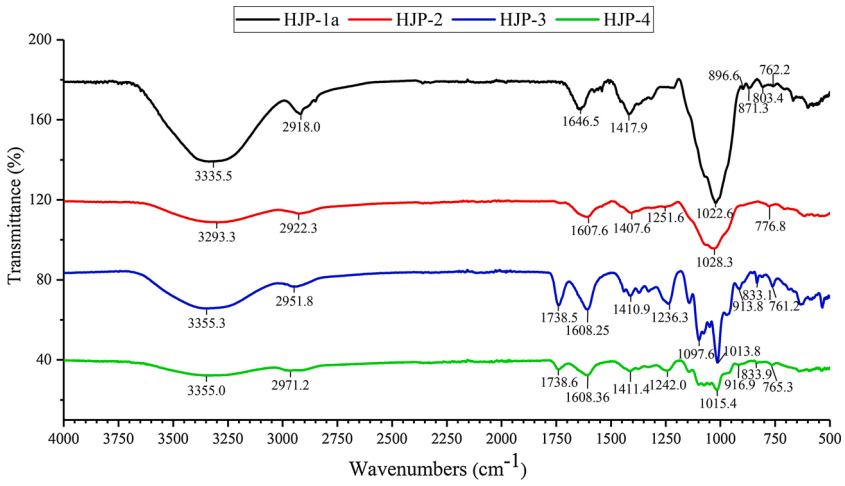

Fig. 2. Fourier-transform infrared spectra of four polysaccharide fractions from *Z. jujuba* cv. *Hamidazao* fruits.

showed the glycosidic linkage pattern in HJP-3, which was the predominant polysaccharide fraction (Figs. S2 and S3). A total of ten derivatives were discovered and identified: 4-Gal*p*A, t-Ara*f*, 5-Ara*f*, 2,4-Rha*p*, 2-Rha*p*, t-Gal*p*, 6-Gal*p*, 3,4-Gal*p*, 4,6-Gal*p* and 3,6-Gal*p*. (1→4)-linked *α*-D-Gal*p*A, (1→)-linked *α*-L-Ara*f* and (1→5)-linked *α*-L-Ara*f* were the most dominant linkage patterns, with a molar ratio of 44.2:17.6:13.3. The results were basically consistent with the monosaccharide composition analysis. Notably, there were also some Rha*p* and Gal*p* residues linked by different types of glycosidic bonds, such as (1→)- and (1→2,4)-linkage. The structure of HJP-3 was further confirmed by NMR spectra.

3.5. NMR spectra analysis of four jujube polysaccharides

The NMR chemical shift data of four jujube polysaccharides revealed the typical characteristics of polysaccharides. As shown in Figs. 3A and S5, the four polysaccharide fractions differed in the signals in the ^{1}H NMR spectra. For HJP-1a, the anomeric proton signals in the ^{1}H NMR spectra were mainly located at δ 4.25–5.50, and peaks in the range of 3.00–4.25 ppm were attributed to the signals of monosaccharide for H-2, H-3, H-4, H-5 and H-6. Furthermore, there was a methyl signal at δ 1.14, which belonged to rhamnose. However, these three sets of signals were distributed at δ 4.20–5.30, δ 3.00–4.20, δ 1.15 for HJP-2, δ 4.40–5.20, δ 3.50–4.37, δ 1.15 for HJP-3 and δ 4.20–5.20, δ 3.20–4.20, δ 1.18 for HJP-4. Considering that HJP-3 was the predominant polysaccharide fraction, a detailed analysis was performed based on one-dimensional and two-dimensional NMR spectra.

In the ^{1}H-NMR spectrum (Fig. 3A), six main anomeric proton signals at δ 5.07, 5.11, 5.09, 4.92, 4.46, and 5.03 appeared in HJP-3, which were labeled as A, B, C, D, E and F, respectively. The strong peaks in the range of 4.37–3.50 ppm were attributed to H-2, H-3, H-4, H-5 and H-6 of *α*-D-Gal*p*A residues. According to the ^{13}C NMR spectrum (Fig. 3B), there were six anomeric signals resonating at δ 107.43/107.40, 107.15/107.08, 99.47, 100.39, 103.20 and 99.58 ppm. These corresponding anomeric carbon signals of labeled residues in the ^{1}H and ^{13}C NMR spectra were assigned with data in the 2D NMR spectra according to the results published in the literature (Ji et al., 2018; Ji et al., 2020; Liu et al., 2020). Based on the chemical shift data in the ^{1}H-^{1}H COSY (Fig. 3C), HSQC (Fig. 3D) and HMBC (Fig. 3E) spectra, the proton and carbon assignments of six main residues in HJP-3 were presented in Table 3. The signal at δ_H 5.07 was derived from the chemical shift of the anomeric proton of residue A, and the corresponding signal in the anomeric carbon was δ_C 107.43/107.40. The δ_C 81.46/δ_H 4.11, δ_C 76.58/δ_H 3.95, δ_C 83.87/δ_H 4.07 and δ_C 67.94 (68.01)/δ_H 3.77 were attributed to C-2, C-3, C-4 and C-5 of residue A, respectively. Similarly, the anomeric protons and carbons of residue B, C, D, E and F produced the signals at δ_C 107.15 (107.08)/δ_H 5.11, δ_C 99.47/δ_H 5.09, δ_C 100.39/δ_H 4.92, δ_C 103.20/δ_H 4.46 and δ_C 99.58/δ_H 5.03. According to these NMR data and the results reported in the literature, we inferred that residue A was assigned as →5)-*α*-L-Ara*f* (1→ (Ji et al., 2018), and residue D, E and F were →4)-*α*-D-Gal*p*A (1→, →4)-*β*-L-Gal*p*A (1→, and →2,4)-*α*-L-Rha*p* (1→, respectively (Ji et al., 2019; Ji et al., 2020; Liu et al., 2020). Furthermore, there were two different terminal signals in HJP-3, which were identified as T-*α*-L-Ara*f* (1→ and T-*β*-D-Gal*p* based on the results of methylation analysis (Ji et al., 2018; Ji et al., 2019). The monosaccharide composition analysis indicated that HJP-3 was mainly composed of galacturonic acid, arabinose, rhamnose and galactose. Therefore, the backbone of HJP-3 appeared to be mainly composed of →4)-*α*-D-Gal*p*A (1→ and →2,4)-*α*-L-Rha*p* (1→ residues with some branches consisting of →5)-*α*-L-Ara*f* (1→ residues and terminals of T-*α*-L-Ara*f* (1→ and T-*β*-D-Gal*p* residues.

There are currently four types of plant pectin, namely, homogalacturonan, rhamnogalacturonan-I (RG-I), rhamnogalacturonan-II (RG-II) and xylogalacturonan. According to the above results, HJP-3 was most likely the type of RG-I, which was different from the pectin reported by Lin et al. (2019).

3.6. Antioxidant activity in vitro

3.6.1. Radical scavenging activity and total reducing capacity

Reactive oxygen species (ROS) are chemically reactive molecules produced during the normal metabolism of the human body, and excessive levels may result in many metabolic disorders and diseases, such as cancer, coronary heart disease, liver injury and hypertension (Ma et al., 2020). Therefore, the balance between the antioxidant defense system and ROS production is crucial to human health (Kang et al., 2015). A lot of studies reported that plant polysaccharides were able to protect the human body from oxidative damage *via* scavenging free radicals and inhibiting lipid peroxidation, such as burdock polysaccharides, garlic polysaccharides and jujube polysaccharides (Liu et al., 2014b; Liu et al., 2020; Pan & Wu, 2014).

As shown in Fig. 4, the four jujube polysaccharide fractions exhibited moderate $ABTS^{+}$ radical scavenging activity in a dose-dependent manner. Increasing the concentration of polysaccharide samples from 0.2 mg/mL to 1.0 mg/mL effectively enhanced the scavenging activity on $ABTS^{+}$ radicals. At the concentration of 1.0 mg/mL, HJP-2 had the highest $ABTS^{+}$ radical scavenging activity (33.2 %), followed by HJP-4 (25.1 %), HJP-3 (18.2 %) and HJP-1a (15.8 %). There was a significant difference between their antioxidant activities of these four polysaccharide fractions ($P < 0.05$). Furthermore, the total reducing capacity of four polysaccharide samples showed an increasing trend with the increase of sample concentration. HJP-2 had the strongest reducing

Table 2
The glycosidic linkage pattern of HJP-3 based on methylation analysis.

Number	RT (min)	Linkage type	Methylated sugars	Molar ratio (%)	Mass fragments (m/z)
1	6.51	t-Ara*f*	1,4-di-O-acetyl-2,3,5-tri-O-methyl arabinitol	19.1	43.0, 71.0, 87.0, 102.0, 118.0, 129.0, 145.0, 161.0
2	9.47	2-Rha*p*	1,2,5-tri-O-acetyl-6-deoxy-3,4-di-O-methyl rhamnitol	2.5	43.0, 72.0, 89.0, 100.0, 131.0, 143.0, 174.0, 190.1, 211.0, 233.9
3	10.67	t-Gal*p*	1,5-di-O-acetyl-2,3,4,6-tetra-O-methyl galactitol	4.0	43.0, 71.0, 87.0, 118.0, 129.0, 145.0, 161.0, 174.0, 205.1, 245.9, 267.1, 303.1
4	11.34	5-Ara*f*	1,4,5-tri-O-acetyl-2,3-di-O-methyl arabinitol	14.5	43.0, 59.0, 87.0, 102.0, 118.0, 129.0, 162.1, 189.0
5	13.22	2,4-Rha*p*	1,2,4,5-tetra-O-acetyl-6-deoxy-3-O-methyl rhamnitol	3.8	43.0, 74.0, 88.0, 117.0, 130.0, 143.0, 160.0, 190.0, 203.1, 256.3, 298.8, 337.9
6	14.58	4-Gal*p*A	1,4,5-tri-O-acetyl-2,3,6-tri-O-methyl galactitol	48.2	43.0, 59.0, 102.0, 118.0, 131.0, 173.0, 201.1, 233.1, 261.1
7	16.33	6-Gal*p*	1,5,6-tri-O-acetyl-2,3,4-tri-O-methyl galactitol	1.4	43.0, 71.1, 87.0, 102.0, 118.0, 129.0, 162.0, 173.1, 189.0, 210.9, 233.1, 270.9, 298.9, 344.9
8	16.63	3,4-Gal*p*	1,3,4,5-tetra-O-acetyl-2,6-di-O-methyl galactitol	2.0	43.0, 59.0, 87.0, 99.0, 118.0, 129.0, 143.0, 185.0, 232.0, 305.0
9	19.63	4,6-Gal*p*	1,4,5,6-tetra-O-acetyl-2,3-di-O-methyl galactitol	1.0	43.0, 75.0, 102.0, 118.0, 141.9, 162.0, 187.0, 211.7, 261.1, 281, 303.9, 340.1
10	19.83	3,6-Gal*p*	1,3,5,6-tetra-O-acetyl-2,4-di-O-methyl galactitol	3.5	43.0, 59.0, 87.0, 118.0, 129.0, 139.0, 160.0, 189.0, 202.0, 234.1, 266.9, 285.9, 305.1, 338.0

powder, and significantly higher than that of the other three polysaccharides ($P < 0.05$). This indicated that HJP-2 could effectively react with free radicals to terminate radical chain reactions. The other three polysaccharide samples also showed moderate reducing capacity. Therefore, different antioxidant activities existed in all four polysaccharide fractions and the acid polysaccharides (HJP-2, HJP-3 and HJP-4) had better radical scavenging activity than that of the neutral polysaccharides (HJP-1a), which was similar to previous research (Wang et al., 2018; Zhang et al., 2017).

The biological activity of polysaccharides depends on their structural characteristics, such as the composition of monosaccharides, molecular weight, glycosidic linkage pattern and conformation of polysaccharides (Wang, Hu, Nie, Yu, & Xie, 2016). The antioxidant activity is positively correlated with the level of uronic acids. The uronic acid contents of HJP-2, HJP-3 and HJP-4 were 70.4 %, 53.8 % and 57.0 %, respectively, which were consistent with the $ABTS^+$ radical scavenging activity and total reducing capacity in the order of HJP-2 > HJP-4 > HJP-3. The molecular weight of polysaccharides is closely associated with their biological activities. The polysaccharides with a low-molecular weight tend to possess strong antioxidant activity due to more reducing hydroxyl groups at their terminals. Moreover, there are other factors that affect the antioxidant activity of polysaccharides. Therefore, the interactions between several structural factors, mainly the monosaccharide composition and molecular weight, determine the biological activities of polysaccharides.

3.6.2. *The protective effect on H_2O_2-damaged HepG2 cells*

The evaluation of antioxidant defense system benefits from the use of several established cell culture lines, such as hepatocellular carcinoma HepG2 cells, human embryonic kidney HEK293 cells and human intestinal Caco-2 cells (Ding et al., 2014; Liu et al., 2014a; Liu, Wang, Tang, Bowater, & Bao, 2019). The HepG2 cell line is a well-differentiated transformed cell line. It shares the phenotypic similarity with normal human hepatocytes and exhibits several advantages (easy to culture, well characterized and highly stable) (Alía, Ramos, Mateos, Bravo, & Goya, 2005). Furthermore, the homeostasis of antioxidant defense in HepG2 cell line is relatively higher than that in hepatocytes and other non-transformed cells. Therefore, it is easier to explore the changes in their responses to different conditions. As presented in Fig. S7, there was no obvious cytotoxicity of jujube polysaccharides to HepG2 cells (2.0–9.7 %) when the polysaccharide concentration was lower than 100 μg/mL. Therefore, three concentrations (25, 50 and 100 μg/mL) were selected to explore the antioxidant activity *in vitro* of jujube polysaccharides based on H_2O_2-induced oxidative stressed HepG2 cells.

As shown in Table 4, the administration of H_2O_2 resulted in an extremely significant decrease in the $OD_{450\ nm}$ in the model group ($P < 0.001$), while Vc and polysaccharide solutions at the concentrations of 25, 50 and 100 μg/mL could effectively relieve this oxidative damage. The best protective effect appeared in the HepG2 cells treated with Vc (100 μg/mL), with an increase of 55.3 % in the cell survival rate compared with the model group ($P < 0.01$). For HJP-1a, HJP-3 and HJP-4, the protective effect of polysaccharides on cell oxidative damage presented an increasing trend as the concentration of the sample solution rose. At 100 μg/mL, the strongest antioxidant activity was observed in HJP-3, resulting in a 51.0 % increase in the $OD_{450\ nm}$, followed by HJP-1a (45.1 %) and HJP-4 (37.3 %), with a significant difference compared with the model group ($P < 0.01$ or 0.05). However, the higher concentrations of HJP-2 caused a lower protective effect on the HepG2 cells. At 25 μg/mL, the $OD_{450\ nm}$ of HepG2 cells increased significantly from 0.532 to 0.799 (increased by 50.8 %) due to the administration of HJP-2 ($P < 0.01$), but the absorbance was only 0.564 when the sample concentration was increased to 100 μg/mL. The protective effect of HJP-2 was significantly higher than those of other polysaccharides (with no significant difference among them, $P > 0.05$) at 25 μg/mL and lower than those of other polysaccharides (with no significant difference among them, $P > 0.05$) at 100 μg/mL. At 50 μg/mL, there was a significant difference between HJP-1a and other three polysaccharides ($P < 0.05$). Notably, the antioxidant activity of HJP was similar to those of HJP-1a and HJP-4, leading to a 14.6 %–40.3 % increase in the $OD_{450\ nm}$ of HepG2 cells at 25–100 μg/mL. Therefore, four purified polysaccharide fractions and crude polysaccharides from *Z. jujuba* cv. *Hamidazao* fruits were able to alleviate the oxidative damage derived from H_2O_2 in HepG2 cells and two acid polysaccharides (HJP-2 and HJP-3) had better antioxidant activity.

3.7. *Antioxidant activity in vivo*

Zebrafish is a tropical freshwater fish and has been widely used to investigate human diseases as an alternative model due to multiple characteristics (small size, large clutch, high transparency, low cost and physiological similarity to mammals) (Kang et al., 2013; Li et al., 2020;

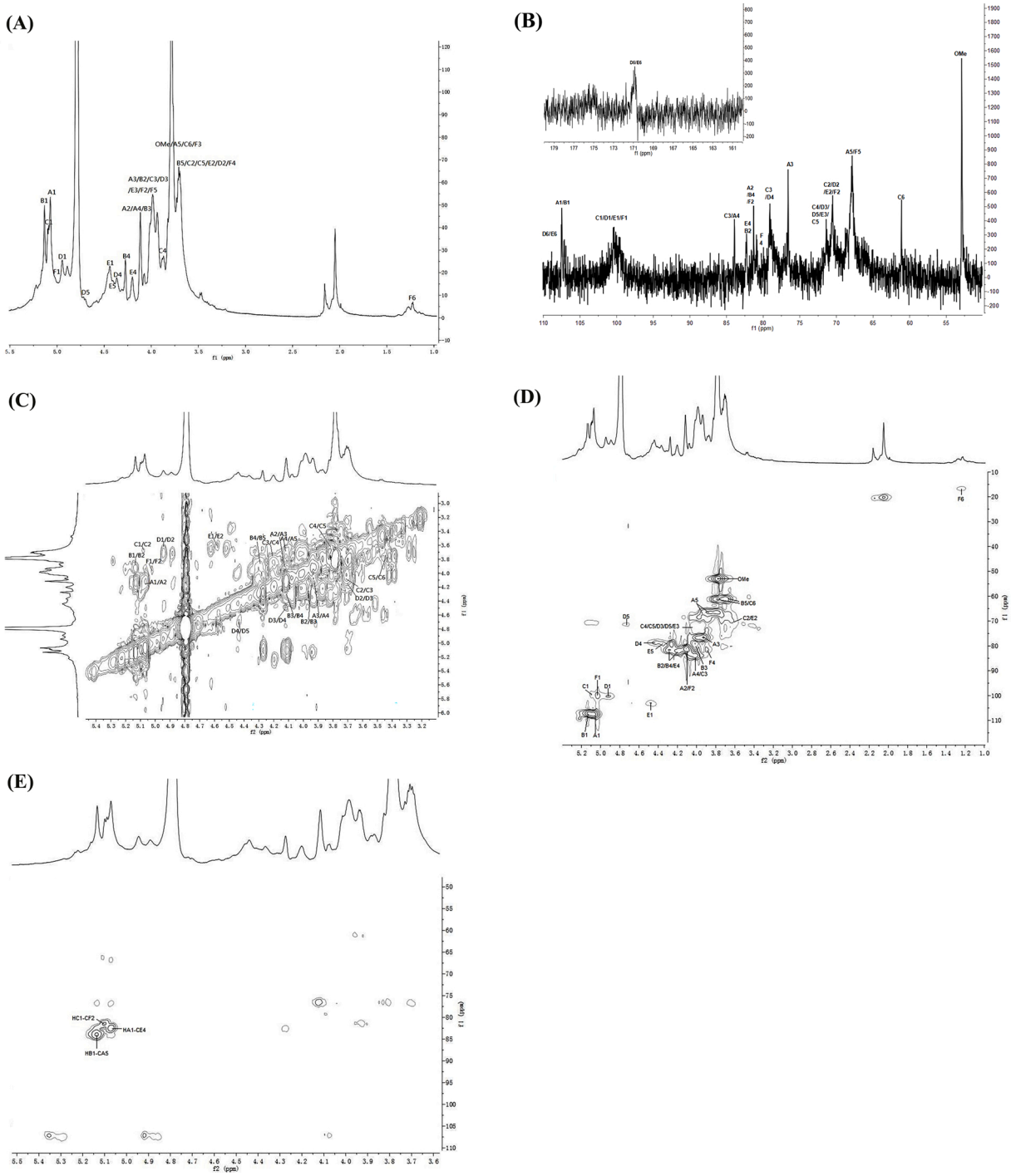

Fig. 3. NMR spectral analysis of HJP-3 from *Ziziphus jujuba* cv. *Hamidazao* fruits. (A) ^{1}H-NMR; (B) ^{13}C-NMR; (C) ^{1}H-^{1}H COSY; (D) HSQC; (E) HMBC.

Wang & Liu, 2020; Zang, Maddison, & Chen, 2018). In particular, the antioxidant activity *in vivo* of a variety of plant polysaccharides was evaluated by oxidative stressed zebrafish (Devi & Viswanathan, 2019; Raguraman et al., 2019; Wang & Liu, 2020). There are many ways to induce oxidative stress in zebrafish, such as 2,2-azobis (2-amidinopropane) hydrochloride (AAPH) (Kang et al., 2014), H_2O_2 (Wang, Fang, & Xiong, 2019) and MET (Kulkarni et al., 2018; Zheng et al., 2020). Although the most serious adverse reactions of MET have been referable to the gastrointestinal tract and convulsive seizures, it also causes severe oxidative damage (Kulkarni et al., 2018). Furthermore, most diseases are caused by or closely related to the imbalance of ROS (Devi & Viswanathan, 2019). Therefore, MET-induced oxidative damage in zebrafish was used to further evaluate the antioxidant activity of the four jujube polysaccharides *in vivo*.

The zebrafish was used to investigate the antioxidant activity *in vivo* of different polysaccharide fractions from *Z. jujuba* cv. *Hamidazao* fruits. As presented in Table 5, the level of fluorescence spots in zebrafish embryos was reduced significantly by 79.1 %–83.3 % due to the administration of MET ($P < 0.001$), but Vc and polysaccharides could protect zebrafish embryos from this oxidative damage and improve their survival rates. The most effective protection against the MET-induced injuries was derived from 100 μg/mL of Vc, leading to a four- to six-fold increase in the survival number, with an extremely significant difference compared with the model group ($P < 0.001$). The treatment of

Table 3
Assignments of ^{1}H and ^{13}C NMR spectra for HJP-3.

			1	2	3	4	5	6
A	→5)-α-L-Araf (1→	C	107.43/107.40	81.46	76.58	83.87	67.94/68.01	–
		H	5.07	4.11	3.95	4.07	3.77	–
B	T-α-L-Araf (1→	C	107.15/107.08	82.13	78.86	81.60	61.13	–
		H	5.11	3.91	4.09	4.27	3.70/3.80	–
C	T-β-D-Galp (1→	C	99.47	69.89	83.93	71.74	72.32	61.13
		H	5.09	3.65	4.02	3.82	3.64	3.78
D	→4)-α-D-GalpA (1→	C	100.39	70.3	71.87	78.63	71.55	170.78
		H	4.92	3.70	4.04	4.43	4.69	–
E	→4)-β-L-GalpA (1→	C	103.20	70.0	72.04	82.25	78.39	170.89
		H	4.46	3.65	4.00	4.22	4.39	–
F	→2,4)-α-L-Rhap (1→	C	99.58	81.30	69.56	80.01	68.45	16.78
		H	5.03	3.95	3.79	3.72	4.02	1.22

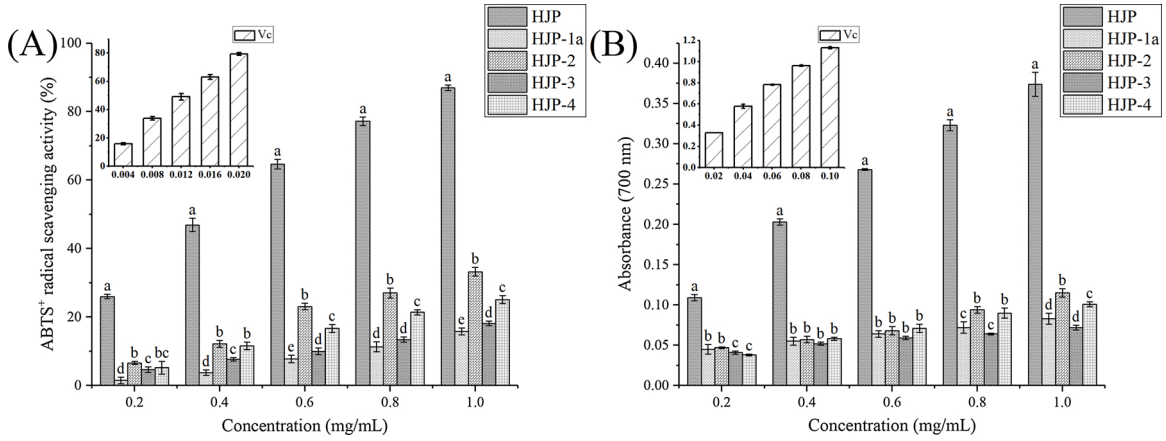

Fig. 4. Antioxidant activity *in vitro* of crude polysaccharides and four purified polysaccharide fractions from *Z. jujuba* cv. *Hamidazao* fruits. (A) $ABTS^{+}$ radical scavenging activity; (B) Total reducing capacity.

Table 4
The protective effect of crude polysaccharides and four purified polysaccharide fractions from *Z. jujuba* cv. *Hamidazao* fruits on H_2O_2-damaged HepG2 cells.

	Blank control	Negative control	Vc	25 μg/mL	50 μg/mL	100 μg/mL
HJP	1.03 ± 0.08^{a}	0.53 ± 0.02^{e}	0.83 ± 0.03^{b}	0.61 ± 0.01^{de}	0.67 ± 0.03^{cd}	0.74 ± 0.04^{bc}
HJP-1a	1.03 ± 0.08^{a}	0.53 ± 0.02^{c}	0.83 ± 0.03^{b}	0.59 ± 0.01^{c}	0.72 ± 0.01^{b}	0.77 ± 0.02^{b}
HJP-2	1.03 ± 0.08^{a}	0.53 ± 0.02^{c}	0.83 ± 0.03^{b}	0.80 ± 0.01^{b}	0.63 ± 0.01^{c}	0.56 ± 0.02^{c}
HJP-3	1.03 ± 0.08^{a}	0.53 ± 0.02^{c}	0.83 ± 0.03^{b}	0.58 ± 0.01^{c}	0.59 ± 0.01^{c}	0.80 ± 0.04^{b}
HJP-4	1.03 ± 0.08^{a}	0.53 ± 0.02^{d}	0.83 ± 0.03^{b}	0.59 ± 0.02^{d}	0.63 ± 0.04^{cd}	0.73 ± 0.04^{bc}

The data were expressed as mean ± standard deviation. Values within the same row followed by different letters are significantly different at $P < 0.05$.

Table 5
The protective effect of crude polysaccharides and four purified polysaccharide fractions from *Z. jujuba* cv. *Hamidazao* fruits on MET-induced oxidative stress in zebrafish.

	Blank control	Negative control	Vc	5 μg/mL	25 μg/mL	50 μg/mL
HJP	120.13 ± 1.38^{a}	25.13 ± 2.12^{c}	106.00 ± 1.01^{ab}	94.00 ± 2.11^{b}	101.25 ± 1.98^{ab}	102.86 ± 1.35^{ab}
HJP-1a	103.00 ± 1.38^{a}	17.17 ± 1.12^{d}	86.00 ± 1.60^{ab}	59.00 ± 2.59^{c}	65.83 ± 1.65^{bc}	74.50 ± 1.95^{bc}
HJP-2	120.13 ± 1.38^{a}	25.13 ± 2.12^{d}	106.00 ± 1.01^{a}	78.75 ± 2.80^{b}	70.88 ± 1.98^{bc}	54.83 ± 2.95^{c}
HJP-3	120.13 ± 1.38^{a}	25.13 ± 2.12^{d}	106.00 ± 1.01^{a}	52.57 ± 2.12^{c}	82.86 ± 1.98^{b}	65.25 ± 1.31^{bc}
HJP-4	120.13 ± 1.38^{a}	25.13 ± 2.12^{c}	106.00 ± 1.01^{a}	63.25 ± 2.88^{b}	56.29 ± 2.86^{b}	67.25 ± 3.03^{b}

The data were expressed as mean ± standard deviation. Values within the same row followed by different letters are significantly different at $P < 0.05$.

crude polysaccharides and four purified polysaccharide fractions from *Z. jujuba* cv. *Hamidazao* fruits also alleviated the oxidative damage induced by MET. The fluorescence spots of zebrafish embryos treated with crude polysaccharides at 25 and 50 μg/mL were similar to those of Vc, showing a higher level of antioxidant activity. Among the four purified polysaccharide fractions, the administration of HJP-1a at 5, 25 and 50 μg/mL resulted in a 60.8 %–83.3 % increase in the fluorescence spots of zebrafish embryos, with a best protective effect against oxidative damage. Furthermore, the survival rate of zebrafish embryos was significantly increased by 71.4 % and 70.7 % when 25 μg/mL of HJP-3 and HJP-2 were provided. In contrast, only 31.2 %–47.1 % of increase in the level of fluorescence points was observed due to the treatment of HJP-4 at 5, 25 and 50 μg/mL, which was considered to have the lowest antioxidant activity. It should be noted that a negative correlation between the protective effect and the concentration of the treated polysaccharide solution appeared in HJP-2, which might be due to the toxicity of high concentrations of polysaccharides to zebrafish embryos. Therefore, crude polysaccharides and four purified polysaccharide fractions from *Z. jujuba* cv. *Hamidazao* fruits showed different protective effects on zebrafish embryos damaged by MET, among which HJP and HJP-1a had better antioxidant activity. The antioxidant activity *in vivo* of polysaccharides was mainly affected by the molecular weight. Low-molecular weight polysaccharides were easily digested, absorbed and metabolized in the body, so they could more effectively protect zebrafish embryos from oxidative damage caused by MET.

4. Conclusion

Four polysaccharide fractions, including one neutral polysaccharide (HJP-1a) and three acid polysaccharides (HJP-2, HJP-3 and HJP-4), were successfully isolated and purified from *Z. jujuba* cv. *Hamidazao* fruits. They differed in monosaccharide composition (mainly mass ratio rather than type) and average molecular weight. HJP-1a was mainly composed of arabinose and galactose in a ratio of 56.9:20.0, with an average molecular weight of 3.115×10^4 g/mol. HJP-2, HJP-3 and HJP-4 were homogeneous heteropolysaccharides mainly containing galacturonic acid, arabinose and galactose, with average molecular weights of 4.590×10^4, 6.986×10^4 and 1.951×10^5 g/mol, respectively. The backbone of HJP-3 appeared to be mainly composed of →4)-*α*-D-Gal*p*A (1→ and →2,4)-*α*-L-Rha*p* (1→ residues with some branches consisting of →5)-*α*-L-Ara*f* (1→ residues and terminals of T-*α*-L-Ara*f* (1→ and T-*β*-D-Gal*p* residues by FTIR, methylation analysis and NMR analysis. Furthermore, different $ABTS^+$ radical scavenging activity and the reducing capacity were observed in the four polysaccharide fractions, in a dose-dependent manner. They also showed excellent protective effect on H_2O_2-induced HepG2 cells and metronidazole-damaged zebrafish embryos, especially HJP-2 *in vitro* and HJP-1a *in vivo*. Therefore, four polysaccharide fractions from *Z. jujuba* cv. *Hamidazao* fruits had significant differences in the structural and antioxidant properties. These results confirmed the antioxidant activity of jujube polysaccharides and provided a theoretical basis for further research on the structure-activity relationship.

CRediT authorship contribution statement

Yanmin Yang: Conceptualization, Methodology, Software, Data curation, Writing - original draft, Visualization, Investigation, Validation. **Zhichang Qiu:** Conceptualization, Methodology, Software, Data curation, Writing - original draft, Visualization, Investigation, Validation. **Lingyu Li:** Data curation, Writing - original draft, Visualization, Investigation. **Sriram K. Vidyarthi:** Data curation, Writing - original draft, Visualization, Investigation. **Zhenjia Zheng:** Conceptualization, Methodology, Software, Supervision, Writing - review & editing. **Rentang Zhang:** Conceptualization, Methodology, Software, Supervision, Writing - review & editing.

Declaration of Competing Interest

The authors report no declarations of interest.

Acknowledgements

This work was supported by the Shandong Key Research and Development Program (2016GNC113015; 2019GNC106061) and Shandong Agricultural Applied Technology Innovation Project (2017).

Appendix A. Supplementary data

Supplementary material related to this article can be found, in the online version, at doi:https://doi.org/10.1016/j.carbpol.2021.117879.

References

Alía, M., Ramos, S., Mateos, R., Bravo, L., & Goya, L. (2005). Response of the antioxidant defense system to tert-butyl hydroperoxide and hydrogen peroxide in a human hepatoma cell line (HepG2). *Journal of Biochemical and Molecular Toxicology, 19*, 119–128.

Bradford, M. M. (1976). A rapid and sensitive method for the quantitation of microgram quantities of protein utilizing the principle of protein-dye binding. *Analytical Biochemistry, 72*, 248–254.

Chang, S. C., Hsu, B. Y., & Chen, B. H. (2010). Structural characterization of polysaccharides from *Zizyphus jujuba* and evaluation of antioxidant activity. *International Journal of Biological Macromolecules, 47*, 445–453.

Chen, J., Li, Z., Maiwulanjiang, M., Zhang, W. L., Zhan, J. Y., Lam, C. T., … Dong, T. T. (2013). Chemical and biological assessment of *Ziziphus jujuba* fruits from China: Different geographical sources and developmental stages. *Journal of Agricultural and Food Chemistry, 61*, 7315–7324.

Devi, D. V., & Viswanathan, P. (2019). Sulphated polysaccharide from *Sargassum myriocystum* confers protection against gentamicin-induced nephrotoxicity in adult zebrafish. *Environmental Toxicology and Pharmacology, 72*, Article 103269.

Ding, L., Zhang, Y., Jiang, Y., Wang, L., Liu, B., & Liu, J. (2014). Transport of egg white ace-inhibitory peptide, Gln-Ile-Gly-Leu-Phe, in human intestinal Caco-2 cell monolayers with cytoprotective effect. *Journal of Agricultural and Food Chemistry, 62*, 3177–3182.

Gao, C. J., Wang, Y. H., Wang, C. Y., & Wang, Z. Y. (2013). Antioxidant and immunological activity *in vitro* of polysaccharides from *Gomphidius* rutilus mycelium. *Carbohydrate Polymers, 92*, 2187–2192.

Gao, Q. H., Wu, C. S., & Wang, M. (2013). The Jujube (*Ziziphus Jujuba Mill.*) fruit: A review of current knowledge of fruit composition and health benefits. *Journal of Agricultural and Food Chemistry, 61*, 3351–3363.

Ji, X. L., Liu, F., Peng, Q., & Wang, M. (2018). Purification, structural characterization, and hypolipidemic effects of a neutral polysaccharide from *Ziziphus Jujuba* cv. *Muzao*. *Food Chemistry, 245*, 1124–1130.

Ji, X. L., Peng, Q., Yuan, Y. P., Shen, J., Xie, X. Y., & Wang, M. (2017). Isolation, structures and bioactivities of the polysaccharides from jujube fruit (*Ziziphus jujuba* Mill.): A review. *Food Chemistry, 227*, 349–357.

Ji, X. L., Yan, Y. Z., Hou, C., Shi, M. M., & Liu, Y. Q. (2020). Structural characterization of a galacturonic acid-rich polysaccharide from *Ziziphus Jujuba* cv. *Muzao*. *International Journal of Biological Macromolecules, 147*, 844–852.

Ji, X. L., Zhang, F., Zhang, R., Liu, F., Peng, Q., & Wang, M. (2019). An acidic polysaccharide from *Ziziphus Jujuba* cv. *Muzao*: Purification and structural characterization. *Food Chemistry, 274*, 494–499.

Kang, M. C., Cha, S. H., Wijesinghe, W. A. J. P., Kang, S. M., Lee, S. H., Kim, E. A., … Jeon, Y. J. (2013). Protective effect of marine algae phlorotannins against AAPH-induced oxidative stress in zebrafish embryo. *Food Chemistry, 138*, 950–955.

Kang, M. C., Kim, S. Y., Kim, E. A., Lee, J. H., Kim, Y. S., Yu, S. K., … Jeon, Y. J. (2015). Antioxidant activity of polysaccharide purified from *Acanthopanax koreanum Nakai* stems *in vitro* and *in vivo* zebrafish model. *Carbohydrate Polymers, 127*, 38–46.

Kang, M. C., Kim, S. Y., Kim, Y. T., Kim, E. A., Lee, S. H., Ko, S. C., … Jang, H. S. (2014). *In vitro* and *in vivo* antioxidant activities of polysaccharide purified from aloe vera (*Aloe barbadensis*) gel. *Carbohydrate Polymers, 99*, 365–371.

Kulkarni, A. A., Conteh, A. M., Sorrell, C. A., Mirmira, A., Tersey, S. A., Mirmira, R. G., … Anderson, R. M. (2018). An *in vivo* zebrafish model for interrogating ROS-mediated pancreatic *β*-cell injury, response, and prevention. *Oxidative Medicine and Cellular Longevity, 2018*.

Li, J., Ai, L., Yang, Q., Liu, Y., & Shan, L. (2013). Isolation and structural characterization of a polysaccharide from fruits of *Zizyphus jujuba* cv. *Junzao*. *International Journal of Biological Macromolecules, 55*, 83–87.

Li, J., Fan, L., & Ding, S. (2011). Isolation, purification and structure of a new water-soluble polysaccharide from *Zizyphus jujuba* cv. *Jinsixiaozao*. *Carbohydrate Polymers, 83*, 477–482.

Li, Y., Li, X., Chu, Q., Jia, R., Chen, W., Wang, Y., … Zheng, X. (2020). *Russula alutacea Fr.* polysaccharide ameliorates inflammation in both RAW264. 7 and zebrafish (*Danio rerio*) larvae. *International Journal of Biological Macromolecules, 145*, 740–749.

Lin, T. T., Liu, Y., Lai, C. J. S., Yang, T. T., Xie, J. B., & Zhang, Y. Q. (2018). The effect of ultrasound assisted extraction on structural composition, antioxidant activity and immunoregulation of polysaccharides from *Ziziphus jujuba* Mill var. *spinosa* seeds. *Industrial Crops and Products, 125*, 150–159.

Lin, X., Ji, X., Wang, M., Yin, S., & Peng, Q. (2019). An alkali-extracted polysaccharide from *Zizyphus jujuba* cv. *Muzao*: Structural characterizations and antioxidant activities. *International Journal of Biological Macromolecules, 136*, 607–615.

Liu, P., Wang, W., Tang, J., Bowater, R. P., & Bao, Y. (2019). Antioxidant effects of sulforaphane in human HepG2 cells and immortalised hepatocytes. *Food and Chemical Toxicology, 128*, 129–136.

Liu, X. X., Liu, H. M., Yan, Y. Y., Fan, L. Y., Yang, J. N., Wang, X. D., & Qin, G. Y. (2020). Structural characterization and antioxidant activity of polysaccharides extracted from jujube using subcritical water. *LWT - Food Science and Technology, 117*, Article 108645.

Liu, J., Chen, Z., He, J., Zhang, Y., Zhang, T., & Jiang, Y. (2014a). Anti-oxidative and antiapoptosis effects of egg white peptide, Trp-Asn-Trp-Ala-asp, against H_2O_2-induced oxidative stress in human embryonic kidney 293 cells. *Food & Function, 5*, 3179–3188.

Liu, W., Wang, J., Zhang, Z., Xu, J., Xie, Z., Slavin, M., & Gao, X. (2014b). *In vitro* and *in vivo* antioxidant activity of a fructan from the roots of *Arctium lappa* L. *International Journal of Biological Macromolecules, 65*, 446–453.

Ma, J. S., Liu, H., Han, C. R., Zeng, S. J., Xu, X. J., Lu, D. J., & He, H. J. (2020). Extraction, characterization and antioxidant activity of polysaccharide from *Pouteria campechiana* seed. *Carbohydrate Polymers, 229*, Article 115409.

Nielsen, S. S. (2010). Phenol-sulfuric acid method for total carbohydrates. *Food analysis laboratory manual* (pp. 47–53). Boston, MA: Springer.

Pan, S., & Wu, S. (2014). Cellulase-assisted extraction and antioxidant activity of the polysaccharides from garlic. *Carbohydrate Polymers, 111*, 606–609.

Raguraman, V., Abraham, L. S., Jyotsna, J., Seedevi, P., Kannan, G. S., Thirugnanasambandam, R., & Kirubagaran, R. (2019). Sulfated polysaccharide from *Sargassum tenerrimum* attenuates oxidative stress induced reactive oxygen species production in *in vitro* and in zebrafish model. *Carbohydrate Polymers, 203*, 441–449.

Ren, G. M., Xu, L. M., Lu, T. Y., & Yin, J. (2018). Structural characterization and antiviral activity of lentinan from *Lentinus edodes* mycelia against infectious hematopoietic necrosis virus. *International Journal of Biological Macromolecules, 115*, 1202–1210.

Tian, Y. T., Zhao, Y. T., Zeng, H. L., Zhang, Y. L., & Zheng, B. D. (2016). Structural characterization of a novel neutral polysaccharide from *Lentinus giganteus* and its antitumor activity through inducing apoptosis. *Carbohydrate Polymers, 154*, 231–240.

Vasilieva, T., Sigarev, A., Kosyakov, D., Ul'yanovskii, N., Anikeenko, E., Chuhchin, D., … Miasnikov, V. (2017). Formation of low molecular weight oligomers from chitin and chitosan stimulated by plasma-assisted processes. *Carbohydrate Polymers, 163*, 54–61.

Vázquez, C. V., Rojas, M. G. V., Ramírez, C. A., Chávez-Servín, J. L., García-Gasca, T., Martínez, R. A. F., … Montemayor, H. M. A. (2015). Total phenolic compounds in milk from different species. Design of an extraction technique for quantification using the Folin–Ciocalteu method. *Food Chemistry, 176*, 480–486.

Wang, W., & Liu, J. (2020). Efficient extraction, antioxidant activities and anti-inflammation of polysaccharides from *Notopterygium franchetii Boiss*. *Carbohydrate Polymers, 248*, Article 116783.

Wang, J., Hu, S., Nie, S., Yu, Q., & Xie, M. (2016). Reviews on mechanisms of *in vitro* antioxidant activity of polysaccharides. *Oxidative Medicine and Cellular Longevity, 2016*, Article 5692852.

Wang, W., Fang, S., & Xiong, Z. (2019). Protective effect of polysaccharide from *Ligusticum chuanxiong hort* against H_2O_2-induced toxicity in zebrafish embryo. *Carbohydrate Polymers, 221*, 73–83.

Wang, Y. G., Xu, Y., Ma, X. Q., Liu, X. F., Yang, M. J., Fan, W. G., & Zhu, X. Q. (2018). Extraction, purification, characterization and antioxidant activities of polysaccharides from *Zizyphus jujuba* cv. *Linzexiaozao*. *International Journal of Biological Macromolecules, 118*, 2138–2148.

Wojdylo, A., Carbonell-Barrachina, A. A., Legua, P., & Hernandez, F. (2016). Phenolic composition, ascorbic acid content, and antioxidant capacity of Spanish jujube (*Ziziphus jujube* Mill.) fruits. *Food Chemistry, 201*, 307–314.

Wu, D. T., Liu, W., Han, Q. H., Du, G., Li, H. Y., Yuan, Q., & Qin, W. (2019a). Physicochemical characteristics and antioxidant activities of non-starch polysaccharides from different kiwifruits. *International Journal of Biological Macromolecules, 136*, 891–900.

Wu, Z., Li, H., Wang, Y. D., Yang, D. J., Tan, H. J., Zhan, Y., & Chen, G. (2019b). Optimization extraction, structural features and antitumor activity of polysaccharides from *Z. jujuba* cv. *Ruoqiangzao* seeds. *International Journal of Biological Macromolecules, 135*, 1151–1161.

Xu, C. L., Qiao, L., Guo, Y., Ma, L., & Cheng, Y. Y. (2018). Preparation, characteristics and antioxidant activity of polysaccharides and proteins-capped selenium nanoparticles synthesized by *Lactobacillus casei* ATCC 393. *Carbohydrate Polymers, 195*, 576–585.

Yuan, Q., Zhao, L., Cha, Q., Sun, Y., Ye, H., & Zeng, X. (2015). Structural characterization and immunostimulatory activity of a homogeneous polysaccharide from *Sinonovacula constricta*. *Journal of Agricultural and Food Chemistry, 63*, 7986–7994.

Zang, L., Maddison, L. A., & Chen, W. (2018). Zebrafish as a model for obesity and diabetes. *Frontiers in Cell and Developmental Biology, 6*, 91.

Zhang, L., Liu, X. Q., Wang, Y. J., Liu, G. P., Zhang, Z., Zhao, Z. X., & Cheng, H. L. (2017). *In vitro* antioxidative and immunological activities of polysaccharides from *Zizyphus Jujuba* cv. *Muzao*. *International Journal of Biological Macromolecules, 95*, 1119–1125.

Zhang, Y., Zhou, T., Wang, H. J., Cui, Z., Cheng, F., & Wang, K. P. (2016). Structural characterization and *in vitro* antitumor activity of an acidic polysaccharide from *Angelica sinensis* (Oliv.) Diels. *Carbohydrate Polymers, 147*, 401–408.

Zheng, L., Ma, Y., Zhang, Y., Meng, Q., Yang, J., Wang, B., … Shi, J. (2020). Increased antioxidant activity and improved structural characterization of sulfuric acid-treated stepwise degraded polysaccharides from *Pholiota nameko* PN-01. *International Journal of Biological Macromolecules, 166*, 1220–1229.

Zou, M., Chen, Y. L., Sun-Waterhouse, D. X., Zhang, Y. H., & Li, F. (2018). Immunomodulatory acidic polysaccharides from *Zizyphus jujuba* cv. *Huizao*: Insights into their chemical characteristics and modes of action. *Food Chemistry, 258*, 35–42.